Penerbit Akademia Baru

Journal of Advanced Research in Fluid Mechanics and Thermal Sciences

Journal homepage: www.akademiabaru.com/arfmts.html
ISSN: 2289-7879

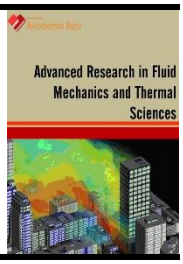

Numerical Studies of In-Cylinder Combustion and Soot Emission Characteristics of Biodiesel Fuels from Different Feedstock

Open Access

Shin Mei Tan[1], Hoon Kiat Ng[1,*], Suyin Gan[2]

[1] Department of Mechanical, Materials and Manufacturing Engineering, University of Nottingham Malaysia, Jalan Broga, 43500 Semenyih, Selangor, Malaysia
[2] Department of Chemical and Environmental Engineering, University of Nottingham Malaysia, Jalan Broga, 43500 Semenyih, Selangor, Malaysia

ARTICLE INFO

Article history:
Received 20 December 2019
Received in revised form 22 February 2020
Accepted 25 February 2020
Available online 24 April 2020

ABSTRACT

Multi-dimensional computation of in-cylinder biodiesel combustion and soot emission characteristics is performed using a commercial Computational Fluid Dynamics (CFD) software, ANSYS FLUENT 13, which is coupled to a chemical kinetic model via a plug-in chemistry solver, CHEMKIN-CFD. To represent the oxygenated straight chain hydrocarbon (HC) of biodiesel, a combined mechanism is utilised by employing the reduced mechanisms of two surrogate fuels, namely methyl butanoate (MB) and n-heptane. The biodiesel fuel types considered in this study include the methyl esters of soy (SME), palm (PME) and coconut (CME), which are modelled by employing the respective thermophysical properties of the fuel and through variation of ratio between MB and n-heptane for accurate representation of its oxygen content. Diesel combustion is also simulated to serve as a benchmark for the study. The computational results indicate that diesel has better combustion efficiency at low engine power with the highest peak of premixed combustion (PMC) and the earliest end of combustion (EOC). As engine power increases, the heat released during PMC is lowered by 30% and the combustion duration are lengthened comparatively. In contrast, biodiesel combustion improves at high power, with CME having the most significant effect whereby the peak heat released rate during PMC improves and the EOC advances to be the earliest among all test fuels. The short HC chain length of CME exerts a more significant effect on the combustion. Comparisons between SME and PME which have similar ignition delays highlight that a high level of unsaturation improves the combustion at low engine power. This effect lessens with increased engine power. At high engine power, the end of PMC and the EOC for SME and PME are similar. The highest level of soot emission is observed for diesel at all levels of engine power followed by SME, PME and CME accordingly.

Keywords:
Biodiesel; Computational Fluid Dynamics; diesel combustion; soot emission

Copyright © 2020 PENERBIT AKADEMIA BARU - All rights reserved

* *Corresponding author.*
E-mail address: hoonkiat.ng@nottingham.edu.my (Hoon Kiat Ng)

https://doi.org/10.37934/arfmts.70.1.4661

1. Introduction

Biodiesel has been gaining popularity as a renewable substitute to fossil diesel fuel due to its compatibility with the existing engine technology and generally lower pollutant emissions. The commonly used vegetable oils for biodiesel production includes soybean oil, rapeseed oil, coconut oil and palm oil [1]. Biodiesel fuels from different feedstock have different effects on the combustion and emission characteristics due to the different fatty acids methyl ester (FAME) compositions. Saturation of the biodiesel fuel components is also a factor influencing the emissions level. Apart from the saturation level, variations in biodiesel emissions are also associated with its oxygen content and physical properties such as viscosity and density which are dictated by the hydrocarbon (HC) chain length [2-5].

The literature has reported that the use of biodiesel in diesel engines is generally linked to reductions in HCs and carbon monoxide (CO) emissions, with trade-offs in power loss and increased fuel consumption [1,6]. Whilst some researchers claim that biodiesel combustion reduces soot or particulate matter (PM) formation, others report contrarily. For instance, certain studies [7-8] found that replacing diesel with biodiesel blends reduced carbon deposition in the combustion chamber. The reduction was attributed to the oxygen content in biodiesel. In contrast, it has also been reported that the use of biodiesel increased the emissions of PM, CO and HC over the New European Driving Cycle (NEDC) as a result of the different physicochemical properties of biodiesel which affected the fuel spray characteristics under varying engine operating conditions [9]. Furthermore, the higher viscosity and lower volatility of biodiesel give rise to problems in spray atomization and mixture formation leading to higher smoke and gummy deposits in the combustion chamber [10].

As such, this study aims to carry out numerical studies of in-cylinder combustion and soot emission characteristics of biodiesel fuels from different feedstock to enhance understanding of biodiesel combustion in compression ignition engines. The motivation behind the selection of biodiesel from different feedstock is to understand the effects of different biodiesel fuel characteristics, specifically saturation level and straight HC chain length, on the combustion and soot emission processes.

2. Methodology

2.1 Computational Mesh and Model Formulations

In this study, numerical computation of a test engine with the specifications shown in Table 1 is conducted using ANSYS FLUENT 12, a commercial CFD software coupled with CHEMKIN-CFD as the chemistry solver. The simulation focuses only on the closed part of the engine cycle, from the intake valve closure (IVC) at -140 crank angle degree (CAD) after top dead centre (ATDC) to the exhaust valve opening time (EVO) at +140 CAD ATDC. As shown in Figure 1, the computational mesh represents 90° sector of the combustion chamber due to the symmetry imposed by the four equally spaced injector nozzle holes. The mesh is created with a cell size of 1.5 mm. Grid independent results were achieved with this setting and further refinement in the resolution was found to give insignificant improvement in the predicted results.

The fuel spray breakup is modelled using the Kelvin-Helmholtz/Rayleigh-Taylor (KH-RT) breakup model. The wall-jet model is applied as the discrete phase boundary condition for the combustion chamber surfaces. Turbulence is solved using the Renormalisation Group (RNG) k-ε turbulence model, and the Standard Wall Function is implemented for the near wall treatment. The chemistry of the surrogate fuel as described later in the Section 2.2 is integrated with the CFD solver through CHEMKIN-CFD. The Eddy-Dissipation Concept (EDC) model is implemented to incorporate the finite-

rate chemistry with turbulent mixing, where the chemical reactions are assumed to occur in fine scales of the small turbulent structure. Predictions of soot formation and oxidation processes are made through the Moss-Brookes soot formation model and the Fenimore-Jones soot oxidation model, respectively. In the Moss-Brookes model, the nucleation of soot precursor, coagulation and surface growth are the variables for the solutions of soot particle concentration and soot mass fraction. Acetylene is considered the most important species for soot formation in diesel combustion [11] and is used to represent the soot precursor species as well as the surface growth species [12]. As proposed by [13], the mass density of soot and the mass of incipient soot particle are fixed at 2000 kg/m^3 and 1200 kg/kmol, respectively for applications involving higher HC fuels. The model constants for the rates of soot inception, coagulation, surface growth and oxidation are set at the values given by [14].

Table 1
Test engine, injector and fuel specifications

Parameter	Specification
Engine type	Light-duty diesel engine
Piston type	Bowl-in-piston
Cylinder head type	Flat cylinder head
Displacement per cylinder (L)	0.347
Compression ratio	19.1
Stroke (cm)	6.9
Bore (cm)	8.0
Piston bowl volume (cm^3)	11.6
Connecting rod length (cm)	11.45
Number of injector holes	4
Nozzle diameter (mm)	0.128
Nozzle nap angle (°)	152
Fuel temperature (K)	312

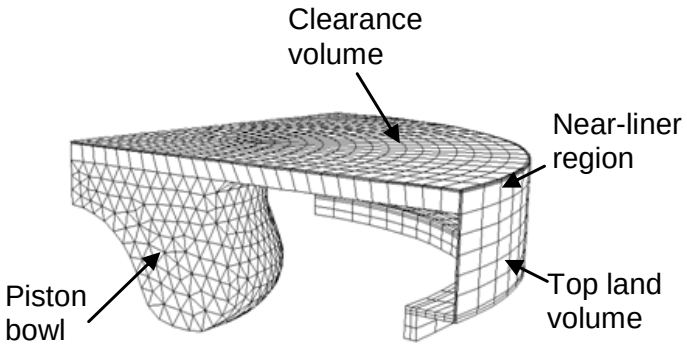

Fig. 1. Computational domain of the combustion chamber

2.2 Operating Conditions and Fuel Injection Parameters

The effects of the fuel types on the combustion processes are examined for a range of engine operating conditions, from low engine power of 0.5 kW to mid and high engine power of 1.5 kW and 2.5 kW, respectively. The engine is maintained at a medium speed of 2000 rpm which is the typical operating range of on-road vehicles and lies within the engine's drivability limits. The test fuels include diesel and three types of biodiesel namely the methyl esters of soy (SME), palm (PME) and coconut (CME), which are the commonly used biodiesels [1]. These fuels are chosen to represent different biodiesel characteristics, namely the saturation level and the straight HC chain length. SME

and PME with similar chain length are used to compare the effects of saturation level since SME is 90% unsaturated while PME is only 50% unsaturated. Meanwhile, CME is studied for its representation of short HC chain length.

The fuel injection system operates with a pressure of 210 bar and a coefficient of discharge value of 0.75. The injection specifications and the operating conditions for each case are summarised in Table 2. The SOI timings marginally vary for different fuel types due to the differences in the bulk modulus, density, viscosity and speed of sound of the fuel. Apart from this, the initial conditions at IVC also vary with different engine powers due to the differences in the temperature of the residual gas in the combustion chamber at the end of each cycle.

Table 2
Injection parameters and operating conditions for varying fuel types at different engine powers

Engine power (kW)	Injection parameter	Diesel	SME	PME	CME
0.5	SOI (CAD ATDC)	-13.5	-15	-15	-16
	EOI (CAD ATDC)	-5.79	-6.29	-6.37	-6.29
	Fuel consumption (kg/h)	0.236	0.274	0.270	0.303
	Total injection quantity (mg/cycle)	3.93	4.57	4.49	5.04
	Initial pressure (bar)	1.23	1.23	1.23	1.23
	Initial Temperature (K)	313	313	313	313
1.5	SOI (CAD ATDC)	-13.5	-15	-15	-16
	EOI (CAD ATDC)	-0.37	1.14	0.42	0.68
	Fuel consumption (kg/h)	0.402	0.508	0.482	0.520
	Total injection quantity (mg/cycle)	6.70	8.46	8.03	8.67
	Initial pressure (bar)	1.27	1.27	1.27	1.27
	Initial Temperature (K)	323	323	323	323
2.5	SOI (CAD ATDC)	-13.5	-15	-15	-16
	EOI (CAD ATDC)	5.74	7.34	7.41	8.49
	Fuel consumption (kg/h)	0.589	0.703	0.700	0.764
	Total injection quantity (mg/cycle)	9.81	11.71	11.67	12.73
	Initial pressure (bar)	1.38	1.38	1.38	1.38
	Initial Temperature (K)	353	353	353	353

2.3 Chemistry and Liquid Properties of Surrogate Fuel Parameters

A combination of methyl butanoate (MB) and n-heptane reaction mechanisms by [15] is utilised as a surrogate fuel model to represent the chemical kinetics of the biodiesel fuel, which is henceforth referred to as the Combined Biodiesel Surrogate (CBS). MB is used to represent the oxygenated content of the FAME while n-heptane represents the straight chain HC. With adjustment to the Arrhenius rate constants, the CBS was successfully validated against both the baseline mechanism in a constant volume adiabatic system at 24 operating conditions relevant to the ignition point of diesel engine. The resulting mechanism consists of 50 species and 201 reactions.

Prior to setting the composition of the simulated fuel, the fatty acids compositions of SME, PME and CME biodiesels are compiled [16-19]. The properties of the biodiesel fuels such as the oxygen content, chemical composition and molecular mass are then determined [15]. In the computation, the chemistry of the biodiesel fuel is represented by the combination of the MB and n-heptane mechanisms while maintaining the oxygen content in the fuel composition. Using the molecular mass, the proportions of MB to n-heptane for each fuel type are calculated. The properties of the experimental biodiesel feedstock and the simulated surrogate fuels are given in Table 3. By preserving the oxygen content of the surrogate fuel to represent the biodiesel fuel, the ratio of

carbon to hydrogen as observed from the chemical composition and the molecular mass are also found to be represented effectively.

Defining the physical properties of the liquid fuel is another important aspect in the setup of the computational modelling of diesel/biodiesel combustion. Due to the differences in the fuel structures such as the saturation level and HC chain length, there are variations in fuel properties. The key properties include density, vapour pressure, heat of vaporisation, liquid heat capacity, liquid dynamic viscosity, liquid thermal conductivity, surface tension and binary diffusivity. The fuel properties of SME, PME and CME utilised in this study have been developed and validated in a constant volume combustion chamber with operating conditions of a compression ignition (CI) engine [20].

Table 3
Properties of simulated surrogate fuels

Type	Properties	SME	PME	CME
Experimental	Chemical composition	$C_{18.8}H_{34.6}O_2$	$C_{18.1}H_{34.9}O_2$	$C_{14.5}H_{29.8}O_2$
	Molecular mass (kg/kmol)	292.5	284.1	234.6
	Oxygen content (wt%)	10.7	11.7	13.5
Simulated	Proportion of MB (wt%)	34.1	35.3	43.0
	Proportion of n-heptane (wt%)	65.9	64.7	57.0
	Chemical composition	$C_{18.8}H_{41.5}O_2$	$C_{18.1}H_{39.9}O_2$	$C_{14.5}H_{31.6}O_2$
	Molecular mass (kg/kmol)	299.5	289.1	237.5

3. Results

3.1 Validation

Validation study is first carried out at three different levels of engine power for every fuel type, i.e. pure diesel, SME, PME and CME. The results of the simulated test cases for variations in engine power are validated against the experimental data, which include the pressure trace, heat released rate (HRR) and tailpipe soot emission as shown in Figure 2 and Figure 3. The comparison between the experimental and simulated results shows that the percentage error in the predicted peak pressure is less than 5.5 %. The over-prediction in the ignition delay (ID) of the main combustion event is maintained to within 18%, which is approximately 2 CAD. Similar HRR curves are also observed between the simulation and experimental data for all cases. With the small offset in the predicted ID, the predictions of the timings of the peak HRR of premixed combustion (PMC) phase are advanced by up to 2 CAD. A possible reason for this observation is that the experimental HRR data itself is often smoothened as reported [21], which increases the width of experimental peak HRR for the PMC phase.

The simulation and experimental exhaust soot concentration are normalised (Figure 3) to the same order of magnitude, by setting the soot amount produced by the case with diesel fuel as the baseline for each engine power. This provides a clear comparison of the trend of soot emission when the fuel type is changed. Although there is discrepancy of up to 21%, the effects of the fuel types on the soot emission are similar in trends for both experimental and simulated results. At the three investigated engine powers, all types of biodiesel produce lower soot levels as compared to diesel. CME produces the least amount of soot followed by PME and SME.

Generally, across all the test cases, the simulated combustion processes and soot emissions agree well with the experimental data, showing that the selected models have been appropriately calibrated for the simulation of this combustion system. Therefore, the combustion and emission characteristics of the three types of biodiesel fuels are well represented by the discrete phase modelling of the fuel liquid properties as well as the reaction mechanism of the surrogate fuel, MB and n-heptane. The above validation exercise indicates the reliability of the model in predicting the

relative progression and development of the in-cylinder processes, including the fuel spray penetration and soot cloud formation.

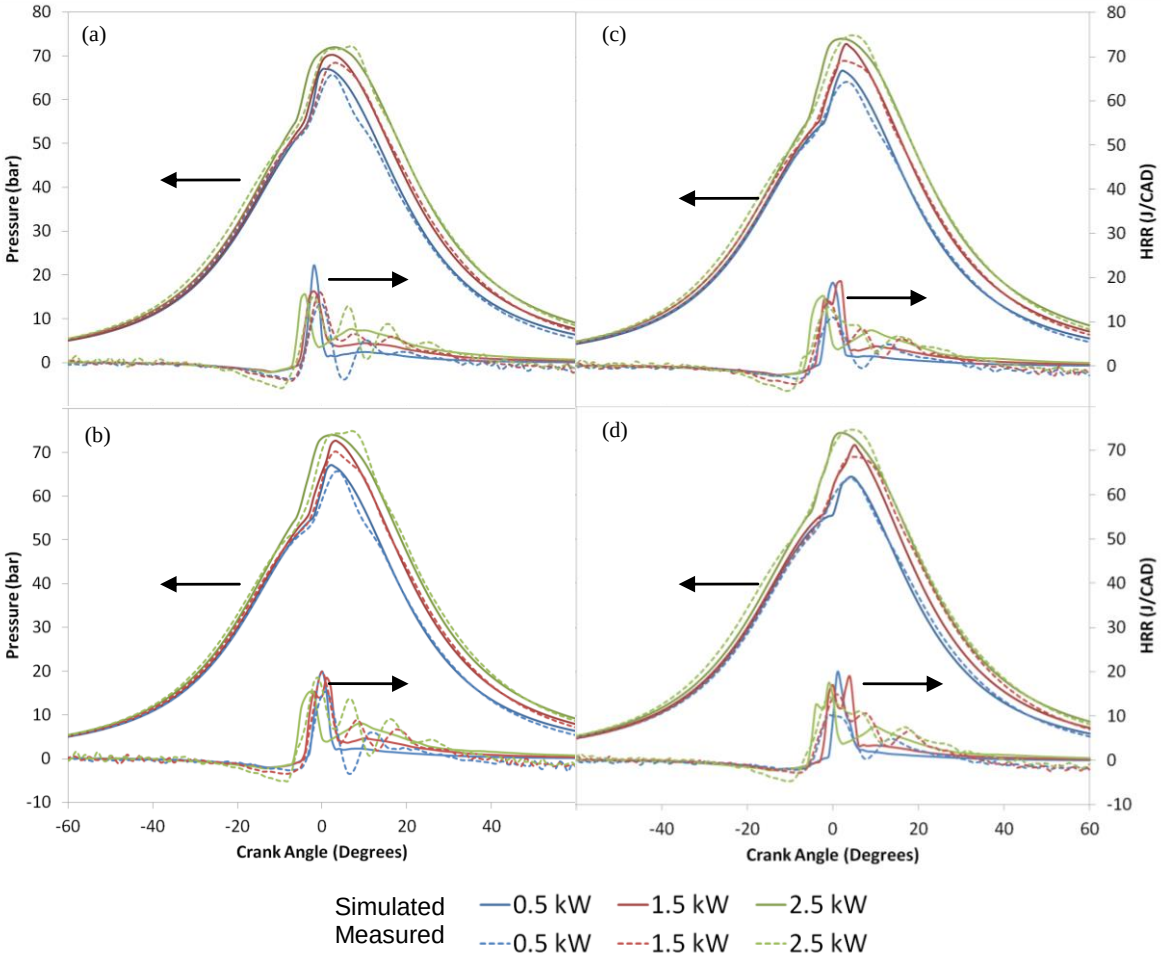

Fig. 2. Measured and simulated pressure and HRR profiles at varying engine power for (a) diesel, (b) SME, (c) PME and (d) CME

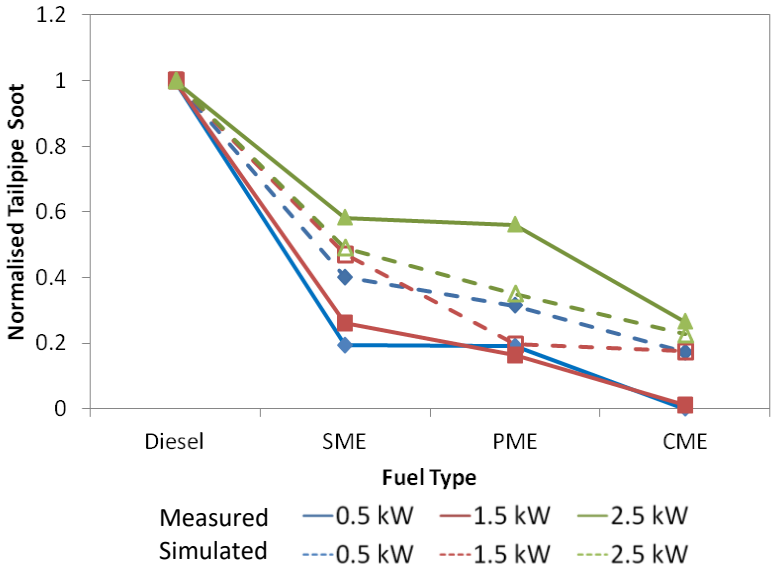

Fig. 3. Normalized tailpipe soot at varying engine power for different fuel types

3.2 Combustion Characteristics

Comparisons of the combustion characteristics are carried out with the data extracted from the simulated pressure and HRR, which includes the ID and the combustion stages of PMC and mixing-controlled combustion (MCC). To obtain the ID, the timing at the onset of positive HRR value is considered to be the start of combustion (SOC). The end of premixed combustion (EOPMC) takes place where the HRR drops to a minimum after the peak of PMC before MCC occurs. The EOC is taken at the point where 90% of the injected fuel is burned. These data are selected for investigation based on the nature of diesel engine combustion, where the thermal efficiency is higher if it approaches the constant volume process, in which combustion takes place instantaneously ATDC [22]. The analysis includes descriptions of the associations between the results with the fuel evaporation rate and the equivalence ratio (ER) of the air-fuel mixture. ER in the combustion chamber at SOC and EOPMC are utilised to illustrate the development of the combustible mixture. Iso-contours of ER value at 0.8 and 1.8 are marked to aid in visualisation as combustion can occur within this region [23].

3.2.1 Overall trends

The results pertaining to the combustion characteristics of different fuel types are presented in Figure 4 and Figure 5. It is observed that the IDs of all fuel types lower as engine power increases. This is attributed to the initial conditions at IVC where the gas temperature and pressure are higher due to the high temperature of the residual gas from the previous cycle produced by a larger amount of fuel burned. Diesel has the shortest ID among all fuels. EOPMC of diesel is advanced compared to biodiesel for all cases, although the peak HRR during PMC and end of combustion (EOC) differ from biodiesel cases at different levels of engine power. Diesel fuel appears to have the best combustion efficiency at low engine power, where it has the highest peak HRR during PMC and the earliest EOC. However, as engine power increases to medium and high level, the heat released during PMC is lower and combustion duration is lengthened comparatively.

SME and PME demonstrate different combustion characteristics at different engine powers, although their IDs are similar. At low power, using SME fuel results in a higher peak HRR during PMC as well as earlier EOPMC and EOC. This remains similar at medium power with earlier EOPMC, but prolonged EOC for SME. The peak HRR during PMC produced by SME drops lower than PME at high engine power. Additionally, high engine power reveals a convergence of the EOPMC and EOC for both the SME and PME cases demonstrating similar combustion characteristics.

The largest ID and the latest EOPMC are observed in the test case of CME combustion. The EOC is retarded when the engine power is low. However, CME shows the best combustion efficiency at high engine power whereby the peak HRR during PMC improves and the EOC advances to be the earliest among all test fuels.

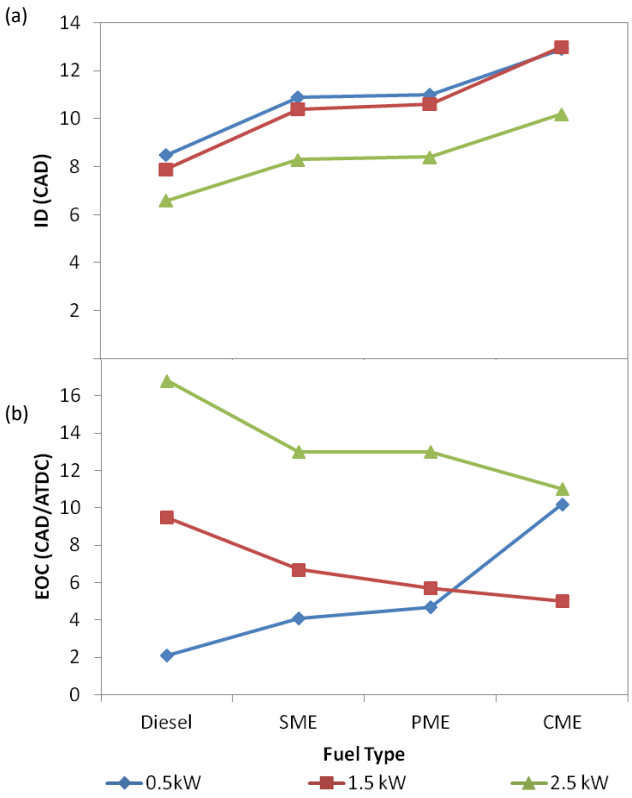

Fig. 4. Combustion characteristics at varying engine power for different fuel types: (a) ID and (b) EOC

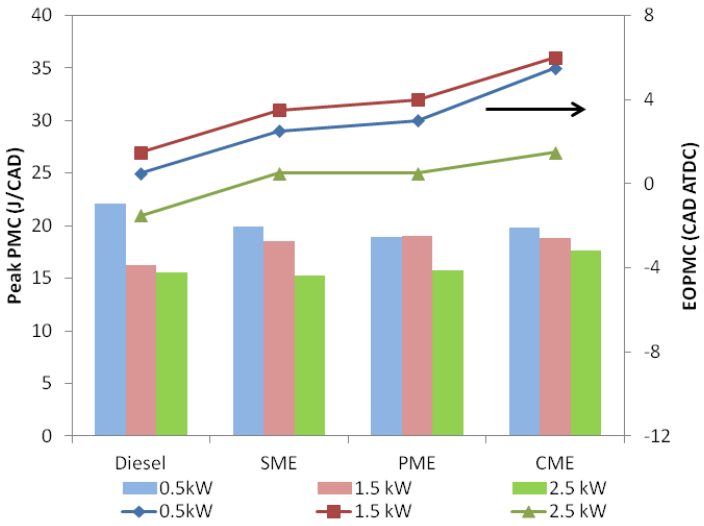

Fig. 5. Combustion characteristics at varying engine power for different fuel types: Peak HRR during PMC and EOPMC

3.2.2 Diesel

The combustion characteristics of diesel fuel are first compared to all biodiesel fuels. Figure 6 shows the evaporation rate of the liquid fuels at all engine powers. The initial evaporation rates are of concern here as they directly affect the IDs. It is observed that within 4 CAD from the SOI, diesel fuel demonstrates the highest evaporation rate which can be attributed to its physical properties of diesel [20]. The surface tension, vapour pressure and density of diesel are at values favourable to

high evaporation rate. Consequently, the combustible mixture prepared by the rapid evaporation of diesel fuel enables it to attain the shortest ID. This deduction is supported by observing the local ER in the combustion chamber in Figure 7. The rich air-fuel mixture of diesel at SOC shows that the ER reaches the optimum level for ignition more rapidly during the ID.

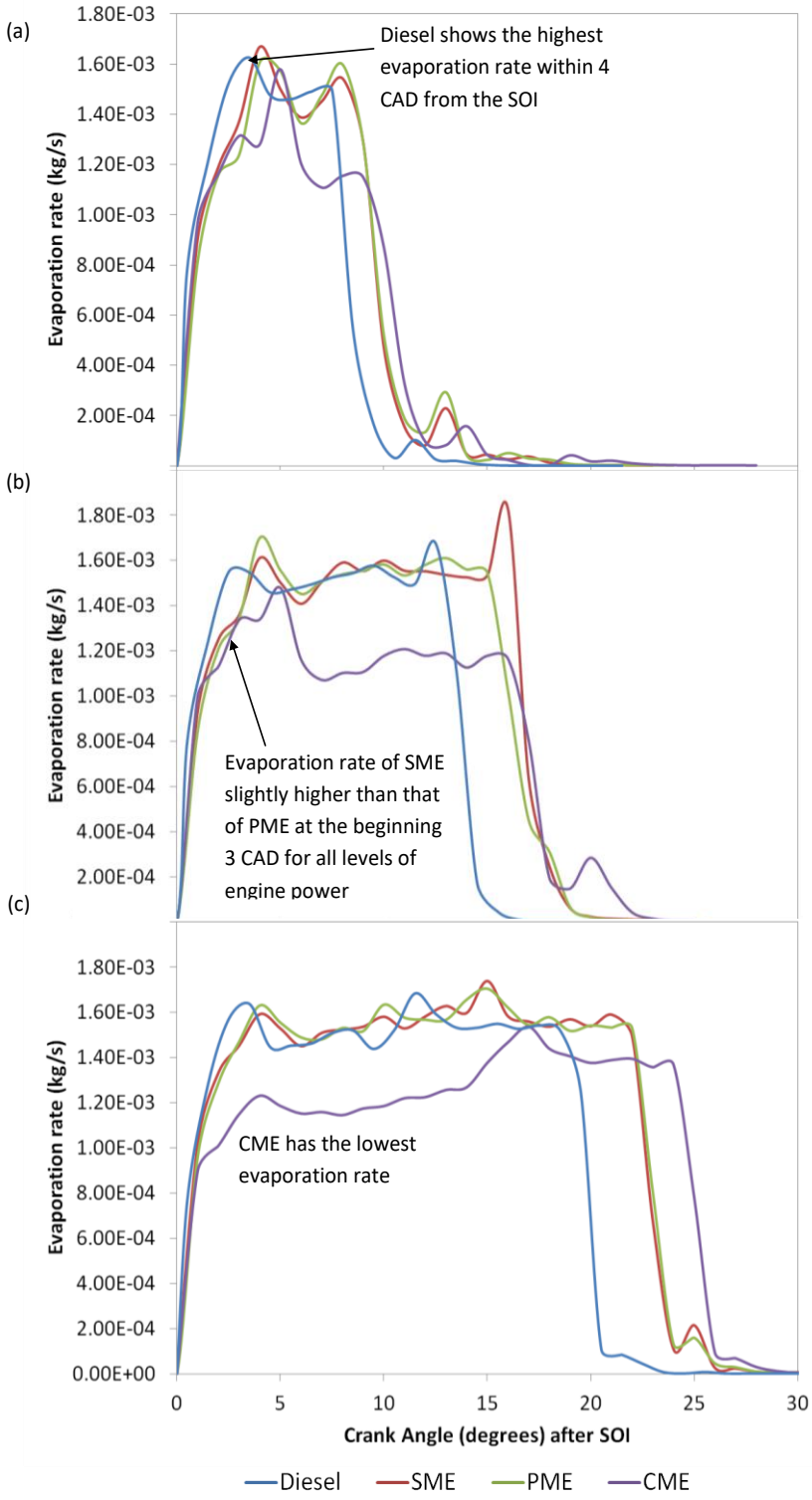

Fig. 6. Fuel evaporation rates for different fuel types at engine power of (a) 0.5 kW, (b) 1.5 kW and (c) 2.5 kW

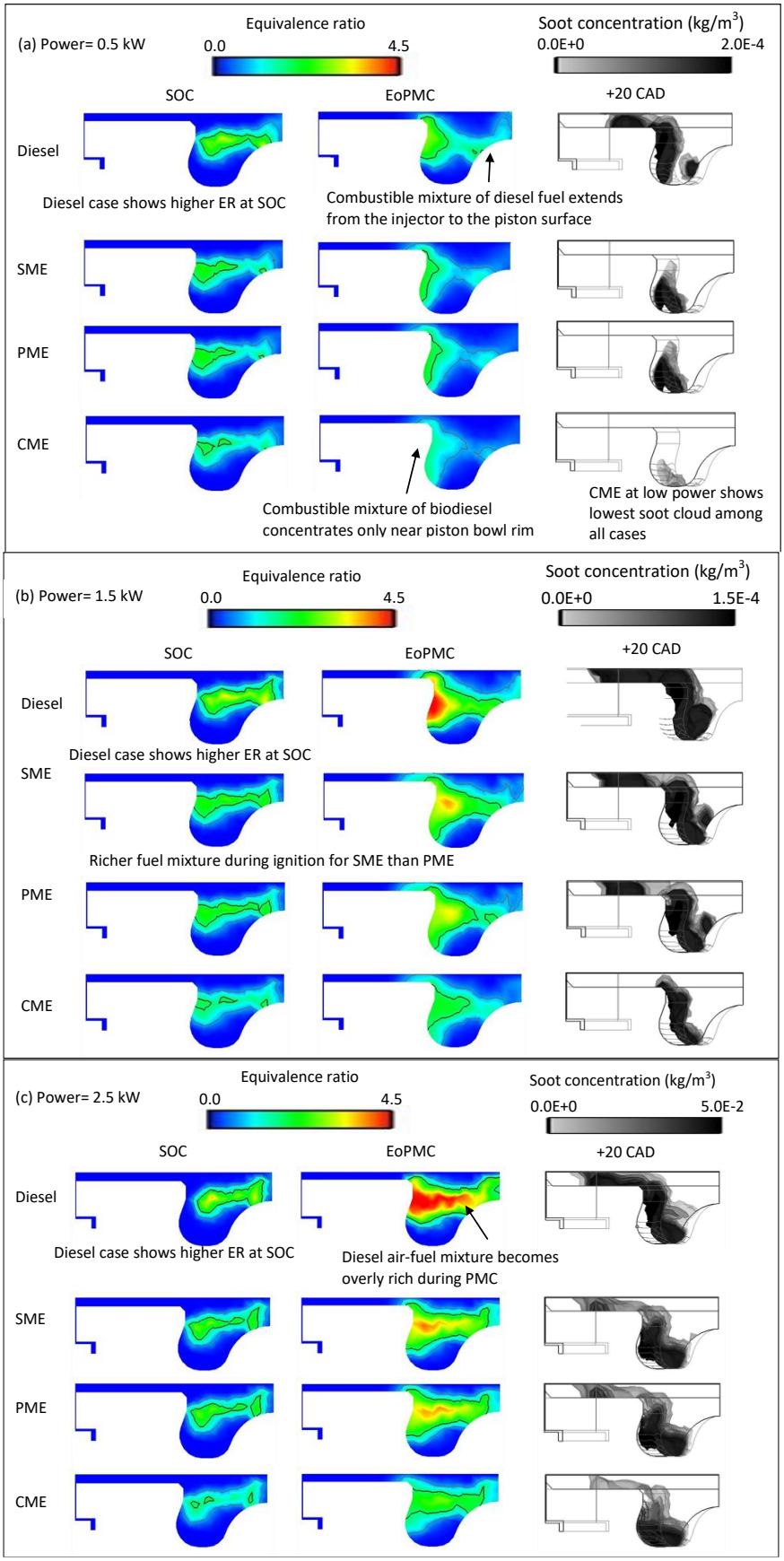

Fig. 7. Contour of ER (left) and soot concentration distributions (right) for different fuel types at SOC and EOPMC: (a) 0.5 kW, (b) 1.5 kW and (c) 2.5 kW

Due to the shortened ID, the heat released is limited by the amount of vaporised fuel at SOC as well as the volume of combustible mixture which is constrained by the undeveloped fuel penetration length. This results in early EOPMC for diesel combustion as compared to other fuels. Conversely, the peak HRR during PMC and EOC of diesel shows variations at different engine powers. At low engine power, the peak of PMC of diesel fuel is the highest as its high evaporation rate results in a volume increase of the combustion region. The combustible mixture of diesel fuel extends from the injector to the piston surface while the mixture of biodiesel fuel at EOPMC concentrates only near the piston bowl rim. Consequently, MCC is improved due to the combined effect of high HRR during the PMC and the early ignition occurring close to TDC. This results in the earliest EOC, where the duration of MCC only sustains for 1.5 CAD.

As engine power increases, the heat released during the MCC stage becomes more prominent. In contrast to low engine power, the peak HRR during PMC of diesel fuel combustion is the lowest among all types of fuels. Subject to the prolonged injection duration, the air-fuel mixture becomes overly rich and suppresses the combustion efficiency. This is illustrated in Figure 7 from the contour of ER at EOPMC. Apart from the high evaporation rate, the rich mixture is also a result of the absence of oxygen content in the diesel fuel as compared to biodiesel. With the short EOPMC and low peak HRR during PMC, the mixing strength of the fuel injected during MCC stage is subsequently deteriorated, therefore delaying the EOC.

3.2.3 Biodiesel

The effects of biodiesel saturation level on combustion characteristics are compared using the cases of SME and PME. Owing to the similarity of oxygen content between these two fuels, the differences in their combustion characteristics are mainly attributed to liquid properties. Although fuel density plays an important role in the atomisation of fuel droplets, the variations between the two biodiesel fuels are less than 2%, which can be considered insignificant as compared to the difference to diesel fuel. The evaporation rate of SME shown in Figure 6 is slightly higher than that of PME at the beginning 3 CAD for all levels of engine power, which is then followed by slight fluctuations at similar magnitudes between the two fuels. At low temperatures, SME has similar vapour pressure as compared to PME, but lower surface tension leading to a higher initial evaporation rate [20].

SME and PME demonstrate different combustion characteristics at different engine powers although their IDs are similar. It is observed from Figure 4 that the MCC phase is not prominent at low engine power. The higher evaporation rate of SME proves to be an advantage when the engine power is low as the maximum local ER of 2 limited by short injection duration promotes complete combustion during the PMC stage. This advances both the EOPMC and EOC. When engine power is increased to 1.5 kW, the duration of combustion is extended during the MCC phase. With increased injection duration, the richer fuel mixture during ignition for SME causes deterioration of PMC as reflected by the lower peak HRR during PMC of 18.5 J/CAD as recorded in Figure 5. In order to compensate for the power loss during PMC, fuel consumption is increased as shown in Table 2. The associated MCC duration is extended, which consecutively delays the EOC.

Both SME and PME show similar combustion characteristics at high engine power. At higher temperatures, the surface tension of PME is lower than that of SME [20]. The initially low evaporation rate of PME is overcome as the fuel injection progresses and the difference between evaporation rates of SME and PME fuel become less evident. As the injection duration increases with engine power, the effects of the initial difference between the fuel evaporation rates on the development of fuel combustion become less significant.

CME is compared against other biodiesel fuels to represent the effects of its short HC chain length on the combustion characteristics. The largest ID and a delayed EOPMC are observed in the combustion of CME. However, CME shows the highest combustion efficiency at high engine power. The evaporation rate of CME is the lowest among the tested fuels as shown in Figure 6, which can be related to its large ID. As CME has the highest oxygen content of 14%, the air-fuel mixture prepared for combustion are leaner as compared to those of other fuels thus delaying the ignition process. This also reduces the amount of chemical heat release within the ID period, causing a lower in-cylinder temperature. Heat transfer to the injected fuel is impeded leading to a low evaporation rate. The low evaporation rate of CME results in an overly lean air-fuel mixture which deteriorates the quality of the combustion and delays both the EOPMC and EOC.

However, as engine power increases, the peak HRR during PMC of CME is improved. The ER of other fuel mixtures becomes too rich for complete combustion while this phenomenon does not occur with CME with its high oxygen content. The EOC of CME also advances to be the earliest among all test fuels. The increasing injection duration extends the fuel delivery to the MCC stage. With less fuel being burned during PMC due to large ID and early EOPMC, the evaporated fuel is carried onto the later stage and creates a more complete combustion in the MCC stage.

In summary, diesel demonstrates better combustion efficiency at low engine power whereas the combustion efficiency of biodiesel fuels improves at high power with CME being the highest. Comparisons between SME and PME demonstrate that a high level of unsaturation improves the combustion at low engine power. The difference in the combustion characteristics between biodiesels of different saturation levels diminishes as the engine power increases. The significant influence of HC chain length on the combustion process is highlighted through the case of CME combustion.

3.3 Tailpipe Soot Emission Characteristics

Figure 3 depicts the normalised tailpipe soot emission produced by different fuel types. The highest level of soot emission is observed for the use of diesel fuel at all levels of engine power. SME produces slightly higher soot level than PME while the combustion of CME results the least amount of soot emission. The ratio between the highest and lowest level of soot produced between the test cases of diesel and CME at the same engine power increases as the engine power decreases. To analyse the soot emission in association with the combustion characteristics in further detail, the net soot level and the soot oxidant, OH radical, are monitored. In addition, the images of predicted soot concentration are shown as side view projections of the 3-D soot iso-surfaces, where the soot cloud layers are featured as semi-transparent. The in-cylinder event at +20 CAD ATDC is chosen for illustration when the combustion processes for all test cases are complete.

3.3.1 Diesel

The results of soot emission are first evaluated for diesel fuel. Figure 8 highlights that diesel combustion produces the highest soot formation rate in all the cases as a result of the high ER in the combustion chamber. With the wide region of rich combustible mixture that extends towards the injector as shown in Figure 7, the combustion region has limited contact area with oxygen which slows down the oxidation process. It is verified by the OH mole fraction illustrated in Figure 8, where the lowest OH concentration is observed in the diesel test case, although the corresponding timespan is longer. The peak of soot oxidation rate in the diesel case appears to be the highest due to the large amount of soot produced, however, it is insufficient to off-set the high soot formation rate.

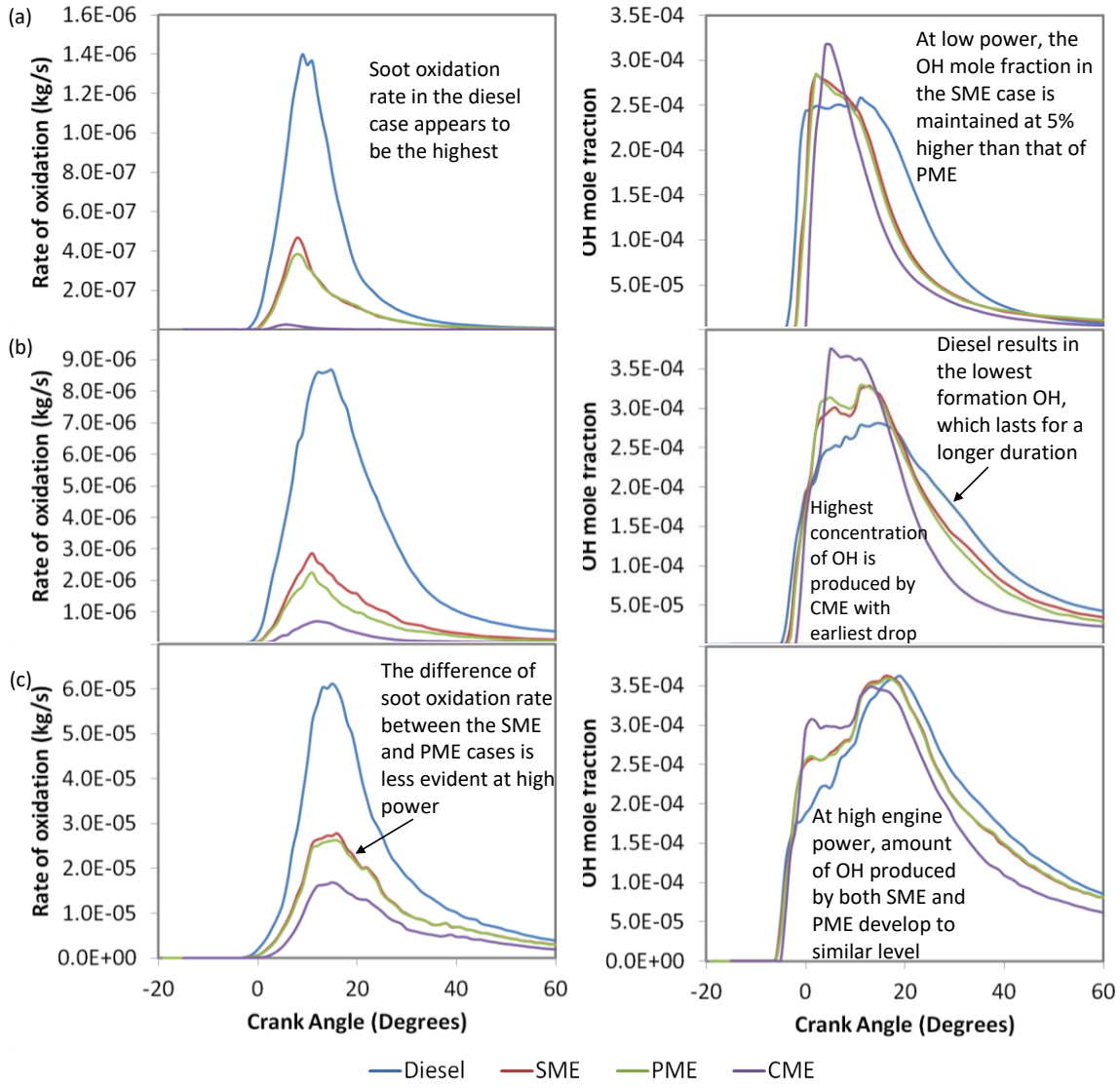

Fig. 8. Rate of oxidation (left) and OH mole fraction (right) for different fuel types at engine power of a) 0.5 kW, (b) 1.5 kW and (c) 2.5 kW

3.3.2 Biodiesel

A comparison of the tailpipe soot emission indicates that SME produces slightly higher soot level than PME. Since both fuel types have similar oxygen content, the difference is mainly attributed to the liquid fuel properties. The rich air-fuel mixture prepared in the event of high evaporation rate of SME fuel droplets provides a higher ER at the point of ignition thus favouring soot formation. In contrast, rapid combustion promotes soot oxidation, ultimately producing a minor difference in the soot level produced by both fuel types. At low power, the OH mole fraction in the SME case is maintained at 5% higher than that of PME during the window of soot oxidation process between +0 and +40 CAD ATDC. At high engine power of 2.5 kW, the amount of OH radicals produced in both SME and PME cases develop to similar levels. Similarly, the difference in soot oxidation rates between the two cases is less evident as observed in Figure 8. This development matches the combustion characteristics of both the fuel types which converge as engine power increases. Therefore, the difference in the soot emission level of the two fuel types is minimal.

Implementation of CME fuel in the diesel engine results in the least amount of soot emission. This is attributed to the high oxygen content of the fuel due to the short HC chain length which results in an air-fuel mixture with low ER for combustion. With oxygen being available in the fuel, the production of the oxidant is increased as seen in Figure 8. The highest concentration of OH after the onset of combustion is produced by CME in all cases. It is also observed that OH level produced by CME has an earlier drop as compared to the other fuel types. As described in Section 4.1.4, owing to the large ID and high oxygen content of CME, a large region of lean air-fuel mixture is created resulting in a wider lean flame region with lower local temperatures. This results in an earlier drop of temperature as well as soot and OH levels.

It is noted that at low engine power, the reduction of tailpipe soot level by replacing diesel fuel with CME is much larger than that of high engine power. This is attributed to the size of the soot cloud produced by CME combustion in the low engine power case, which is much smaller in comparison to the other fuel types. The surface area-to-volume ratio is reduced significantly and this increases the availability of oxidants for soot oxidation.

4. Conclusions

In this study, integrated chemical kinetic modelling with CFD has been used to investigate in-cylinder combustion and soot emission characteristics of biodiesel fuels from different feedstock. Diesel demonstrates better combustion efficiency at low engine power with the highest peak of PMC and earliest EOC. As engine power increases, the heat released during PMC is lowered by 30% and combustion duration are lengthened comparatively. The combustion of biodiesel fuel improves at high power, with CME having the most significant effect where the peak HRR during PMC improves and the EOC advances to be the earliest among all test fuels. CME demonstrates that the HC chain length results in a more significant effect on the combustion. Comparisons between SME and PME show that a high level of unsaturation improves the combustion at low power although their IDs are similar, and this effect diminishes as engine power increases. The EOPMC and EOC for both fuels become similar at high engine power. The highest level of soot emission is observed for the employment of diesel fuel at all levels of engine power. SME produces slightly higher soot level than PME whereas CME results in the least amount of soot emission.

Acknowledgements

The Ministry of Higher Education (MOHE) Malaysia is acknowledged for its financial support towards this work under the Fundamental Research Grant Scheme (FRGS) FRGS/1/2014/TK01/UNIM/01/1.

References

[1] Demirbaş, Ayhan. "Progress and recent trends in biodiesel fuels." *Energy Conversion and Management* 50, no. 1 (2009): 14-34. https://doi.org/10.1016/j.enconman.2008.09.001

[2] Cardone, Massimo, Maria Vittoria Prati, Vittorio Rocco, Maurizia Seggiani, Adolfo Senatore, and Sandra Vitolo. "*Brassica carinata* as an alternative oil crop for the production of biodiesel in Italy: engine performance and regulated and unregulated exhaust emissions." *Environmental Science and Technology* 36, no. 21 (2002): 4656-4662. https://doi.org/10.1021/es011078y

[3] Di, Yague, C.S. Cheung, and Zuohua Huang. "Experimental investigation on regulated and unregulated emissions of a diesel engine fueled with ultra-low sulfur diesel fuel blended with biodiesel from waste cooking oil." *Science of the Total Environment* 407, no. 2 (2009): 835-846. https://doi.org/10.1016/j.scitotenv.2008.09.023

[4] Hossain, Abul Kalam and Philip A. Davies. "Plant oils as fuels for compression ignition engines: a technical review and life-cycle analysis." *Renewable Energy* 35, no. 1 (2010): 1-13.

https://doi.org/10.1016/j.renene.2009.05.009
[5] Janaun, Jidon and Naoko Ellis. "Perspectives on biodiesel as a sustainable fuel." *Renewable and Sustainable Energy Reviews* 14, no. 4 (2010): 1312-1320. https://doi.org/10.1016/j.rser.2009.12.011
[6] Xue, Jinlin, Tony E. Grift, and Alan C. Hansen. "Effect of biodiesel on engine performances and emissions." *Renewable and Sustainable Energy Reviews* 15, no. 2 (2011): 1098-1116. https://doi.org/10.1016/j.rser.2010.11.016
[7] Agarwal, Avinash Kumar, Jayashree Bijwe, and L.M. Das. "Effect of biodiesel utilization of wear of vital parts in compression ignition engine." *Journal of Engineering for Gas Turbines and Power* 125, no. 2 (2003): 604-611. https://doi.org/10.1115/1.1454114
[8] Reksowardojo, Iman K., Ngoc Dung Nguyen, Q.T. Tran, R. Sopheak, Tirto P. Brodjonegoro, Tatang H. Soerawidjaja, H. Ogawa, and W. Arismunandar. "The comparison the effect of biodiesel fuel from palm oil and physic nut oil (*Jatropha curcas*) on an direct injection (DI) diesel engine." In *Proceedings of FISITA 2006 conference in Yokohama, Japan.* 2006.
[9] Fontaras, Georgios, Georgios Karavalakis, Marina Kousoulidou, Theodoros Tzamkiozis, Leonidas Ntziachristos, Evangelos Bakeas, Stamoulis Stournas, and Zissis Samaras. "Effects of biodiesel on passenger car fuel consumption, regulated and non-regulated pollutant emissions over legislated and real-world driving cycles." *Fuel* 88, no. 9 (2009): 1608-1617. https://doi.org/10.1016/j.fuel.2009.02.011
[10] Ng, Jo-Han, Hoon Kiat Ng, and Suyin Gan. "Advances in biodiesel fuel for application in compression ignition engines." *Clean Technologies and Environmental Policy* 12, no. 5 (2010): 459–493. https://doi.org/10.1007/s10098-009-0268-6
[11] Kong, Songcharng, Yong Sun, and Rolf D. Reitz. "Modeling diesel spray flame liftoff, sooting tendency, and NO_x emissions using detailed chemistry with phenomenological soot model." *Journal of Engineering for Gas Turbines and Power* 129, no. 1 (2007): 245-251. https://doi.org/10.1115/1.2181596
[12] Pang, Kar Mun, Hoon Kiat Ng, and Suyin Gan. "Simulation of temporal and spatial soot evolution in an automotive diesel engine using the Moss-Brookes soot model." *Energy Conversion and Management* 58, (2012): 171-184. https://doi.org/10.1016/j.enconman.2012.01.015
[13] Hall, R. J., M. D. Smooke, and M. B. Colket. "Predictions of soot dynamics in opposed jet diffusion flames." *Physical and Chemical Aspects of Combustion: A Tribute to Irvin Glassman* 4 (1997): 189-229.
[14] Moss, J., S. Perera, C. Stewart, and M. Makida. "Radiation heat transfer in gas turbine combustors." In *Proc 16th (Int'l) Symp on Airbreathing Engines, Cleveland, OH*. 2003.
[15] Tan, Shin Mei. "CFD Modelling of Soot Entrainment via Thermophoretic Deposition and Crevice Flow in CI Engines Fuelled with Diesel-Biodiesel Fuel Blends." PhD Thesis, University of Nottingham Malaysia, 2015.
[16] Demirbaş, Ayhan. "Biodiesel fuels from vegetable oils via catalytic and non-catalytic supercritical alcohol transesterifications and other methods: a survey." *Energy Conversion and Management* 44, no. 13 (2003): 2093-2109. https://doi.org/10.1016/S0196-8904(02)00234-0
[17] Demirbaş, Ayhan. "Biodiesel production from vegetable oils via catalytic and non-catalytic supercritical methanol transesterification methods." *Progress in Energy and Combustion Science* 31, no. 5-6 (2005): 466-487. https://doi.org/10.1016/j.pecs.2005.09.001
[18] Graboski, Michael S. and Robert L. McCormick. "Combustion of fat and vegetable oil derived fuels in diesel engines." *Progress in Energy and Combustion Science* 24, no. 2 (1998): 125-164. https://doi.org/10.1016/S0360-1285(97)00034-8
[19] Ng, J-H., Hoon Kiat Ng, and Suyin Gan. "Recent trends in policies, socioeconomy and future directions of the biodiesel industry." *Clean Technologies and Environmental Policy* 12, no. 3 (2010): 213-238. https://doi.org/10.1007/s10098-009-0235-2
[20] Ismail, Harun Mohamed, Hoon Kiat Ng, Xinwei Cheng, Suyin Gan, Tommaso Lucchini, and Gianluca D'Errico. "Development of thermophysical and transport properties for the CFD simulations of in-cylinder biodiesel spray combustion." *Energy & Fuels* 26, no. 8 (2012): 4857-4870. https://doi.org/10.1021/ef300862u
[21] Brakora, Jessica L., Youngchul Ra, Rolf D. Reitz, Joanna McFarlane, and C. Stuart Daw. "Development and validation of a reduced reaction mechanism for biodiesel-fueled engine simulations." *SAE International Journal of Fuels and Lubricants* 1, no. 1 (2009): 675-702. https://doi.org/10.4271/2008-01-1378
[22] Gupta, Hari N. *Fundamentals of Internal Combustion Engines*. Prentice-Hall Of India Pvt. Limited. 2006.

[23] Pulkrabek, Willard W. *Engineering Fundamentals of the Internal Combustion Engine*. Pearson Prentice Hall. 2004.